ANNALS OF GEOPHYSICS, 66, 5, 2023; doi:10.4401/ag-8837
OPEN ACCESS

Monitoring the vegetation stress coming from anthropogenic activities by modeling phenology using Sentinel-2 data

Giuseppe Mancino[*,1], Rodolfo Console[1], Michele Greco[2], Maria Lucia Trivigno[1] and Antonio Falciano[1]

(1) Centro di Geomorfologia Integrata per l'Area del Mediterraneo, Via F. Baracca 175, 85100 Potenza, Italy
(2) Engineering School, University of Basilicata, 85100 Potenza, Italy

Article history: received May 2, 2022; accepted March 14, 2023

Abstract

The study aimed at verifying the existence of stress induced on the functionality of natural ecosystems by particularly impacting anthropogenic activities. In detail, a methodology has been developed to evaluate any alterations in the phenology of plant species in areas surrounding sites defined by Italian legislation as "potentially polluted". Specifically, the study areas located in Basilicata (southern Italy) were intended for municipal solid waste management activities and, at some stage of their management, Potential Toxic Elements (PTEs) concentrations were recorded above the thresholds permitted by the current legislation. The phenological trends of the vegetation were analyzed at gradually increasing distances from the centroid of the sites and then compared with points of the same type of vegetation, very distant from the sites, in areas that were not reasonably impacted by any contamination. The reconstruction of the phenological trends was carried out using Sentinel-2 images approximately on a monthly basis from which the Normalized Difference Vegetation Index (NDVI) was evaluated. Finally, the trends between areas adjacent the sites and unpolluted ones were statistically analyzed using dissimilarity indices which led to the conclusion of the non-existence of effects induced by PTEs on the functionality of the vegetation.

Keywords: Forest decline; Sentinel-2; Environmental stress; Phenology; Dissimilarity indices

1. Introduction

Since the 1970s, the degradation and death of trees and forests have been reported from all continents [Schutt and Cowling, 1985; McLaughlin, 1985; Clauser and Gellini, 1986, Cowling, 1986; Fluckiger et al., 1986; Kozlowski and Costantinidou, 1986; Krause et al., 1986; Gartner, 1987; Ciesla et al., 1994]. Specifically, the correlation between this vegetation decline and pollution phenomena was experienced in Germany towards the end of the seventies, when the term "*Waldsterben*" (forest death) was coined to describe the forest decay that was happening especially in the south of that country [Innes, 1993].

Subsequently, the terminology that correlates forest decay with pollution phenomena was updated with the term "new type of forest damage" ("*Neuartige Waldschäden*"). A synergy of factors certainly contributes to causing this large-scale deterioration of forests, but in which the role of potentially toxic elements (PTEs) has already been highlighted by various authors [Johnson et al., 1990; Burton et al., 1986; Friedland et al., 1986; Hagemeyer and Breckle, 1996; Herrick and Friedland, 1991]. PTEs, although present in a natural way, are introduced into the ecosystem in large quantities as a result of anthropic activities, mainly due, in recent decades, to the population explosion and the significant increase in industrialization processes [Jimenez-Ballesta et al., 2017; Petrotou et al., 2012]. Mining activities [Odumo et al., 2014; Boularbah et al., 2006], the use of fossil fuels [Karbassi et al., 2015; Rodríguez Martín et al., 2015], the industrial [Lv et al., 2015; Rodríguez Martín and Nanos, 2016] and agricultural sectors [Mirsal, 2004], waste disposal [Ghosh e Singh, 2005; Zhang and Hang, 2009; Guerrero et al., 2013; Igbinomwanhia and Ideho; 2014; Steffan et al., 2018] are the activities that most introduce heavy metals (HMs) into the environment. Often these elements persist over time, giving rise to bioaccumulation phenomena and causing stress, even after the cessation of human activities, which materialize in symptoms of suffering of living organisms [Kancheva and Borisova, 2007; Kancheva et al., 2005]. The latter result in alterations of communities, populations, organisms or parts or functions of living organisms [Bussotti and Ferretti; 1998]. HMs are in fact absorbed by plants and often, depending on the species and type of chemical element [Cheng, 2003; Rahman et al., 2007], accumulate in them causing problems not only for vegetation but also for human health if the bioaccumulation concerns species of food interest [Milton et al., 1989; Su et al., 2007; Sridhar et al., 2007; Shiyab et al., 2009]. HMs, in particular Cr, Mn, Fe, Ni, Cu, Zn, Cd, Pb, and Hg, [Brimer, 2011], can cause well-known problems in plants [Demirevska-Kepova, 2004; Xiong et al. 2014; Mathur et al., 2016; Mera et al., 2016; Ivanov et al., 2016; Pierart et al., 2015; Zaanouni et al., 2018]. As, Pb, Cd and Hg, in particular, due to their high toxicity, frequency, and possibility of exposure to humans, are considered the elements of greatest danger [Arun et al. 2005; Singh and Kalamdhad 2011; Sabir et al. 2015; Liu et al., 2015].

The toxicity of HMs in plants has been widely documented for both natural herbaceous species and pastures [Llewellyn et al., 2001; Kooistraa et al., 2004; Minkina et al., 2008; Chaplygin et al., 2018], and cultivated species of food interest [Schreck et al. 2012; Austruy et al. 2013; Mandzhieva et al., 2016; Rahman et al., 2007; Wang and Liu, 2018; Liu et al., 2018]. There is also extensive documentation of the damage caused by HMs in shrub and tree species [Khalili et al., 2015; Martin et al., 2018].

Tree species can be considered an excellent tool for biomonitoring of metals due to their continuous growth, high biomass, extensive root system and low impact on the food chain and human health [Estrabou et al., 2011; Kovalchuk et al., 2001; Singh et al., 2005; Stankovic and Stankovic, 2013; Xu et al., 2014; Temmerman et a al., 2005; Patel et al., 2015].

The accumulation of HMs in tree leaves has been proposed by various authors to assess the quality of the environment and bioaccumulation flows [Tomaševič et al., 2008; Liu et al., 2007; Massadeh et al., 2009; Piczak et al., 2003; Napa et al., 2017], so much that the use of trees as bioindicators was already known at the beginning of the 70s [Smith, 1970].

The alterations caused on plants by high concentrations of HMs range from modifications of the protein and enzymatic structure of the cell membrane [Singh et al., 2015], to variations in the mechanisms of root absorption, to the alteration of the accumulation processes of reserve substances during germination [Wani et al., 2008]. These changes in biochemical processes ultimately result in changes in photosynthetic and transpiration processes [Carlson et al., 1975; Farooqui et al., 1995; Ekmekci et al., 2005] which in turn are expressed in morphological alterations ranging from the reduction of the leaf surface to the early fall of the leaves, to the increase in the crown transparency, and to the more frequent phenomena of chlorosis [Chatterjee and Chatterjee, 2000; Kabata-Pendias, 2007; Chen et al., 2008; Lausch et al., 2017, 2018]. HMs also interfere with photosynthetic and respiratory processes, with nitrogen metabolism and the absorption of water and nutrients [Shahid et al., 2011, 2012, 2013, 2014; Austruy et al. 2014; Hasanuzzaman et al., 2014], causing a reduction in the growth of both the hypogeal and epigeal part of plants [Zouari et al., 2016a e 2016b].

All these effects induced on the vegetation by the presence of high concentrations involve variations in the spectral reflectance characteristics of the leaves and crown, especially in the ranges of the electromagnetic spectrum interested in photosynthetic processes [Liu et al., 2012; Sanches et al., 2014 Huang et al., 2015] and in the near-infrared. Therefore, by exploiting multispectral [Dunagan et al., 2007; Guan and Liu; 2009; Chi et al., 2011; Scudiero et al., 2015; Liu et al., 2016; Zhou et al., 2017] or hyperspectral data [Fu et al., 2013; Liu et al., 2010; Rumpf et al., 2010; Liu et al., 2011], satellite remote sensing (RS) can identify the morphological and functional

variations induced on the vegetation by contamination due to PTEs [Li et al., 2008; Choe et al., 2008; Chi et al, 2011; Liu et al., 2017; Jin et al., 2017]. The traditional methods of identifying potential pollution, based on field surveys on soil and vegetation and subsequent laboratory analyzes, are very expensive and not applicable to large areas [Jin et al., 2015]. Therefore, RS represents a valid alternative method for monitoring any effects induced by contamination [Wei et al., 2013, Liu et al., 2015; Ren et al., 2008], being able to explore very large areas concerning the source of pollution and on a regular and very dense matrix (depending on the spatial resolution of the satellite image) and not simply on the few points of survey on the ground, usually very close to the source of pollution, according to the classical analyses. Vegetation Indices (VIs), namely the combination of two or more spectral bands in such a way as to minimize variations due to external factors, are often used for the analysis of vegetation variations [Huete, 1988; Broge and Leblanc, 2000; Ji and Peters, 2006; Zhang et al., 2018; Mancino et al., 2020; Zu et al., 2021] enhancing the reflectance of the vegetation. NDVI is the best known and widely tested VI capable of evaluating the parameters that are influenced by the presence of contaminants: chlorosis, phylloptosis with a consequent increase in the crown transparency, reduction of growths and biomass, etc. [Peñuelas et al., 1998; Slaton et al., 2001; Liu et al., 2017; Jin et al., 2017]. The models generally used are empirical or semi-empirical and correlate the spectral response of bands or VIs with the physiological or morphological conditions of plants [Liu et al., 2018], at a certain time of the year. Various studies in recent years have shown how the variations induced by PTE contamination can vary during the phenological cycle of plants [Wang et al., 2007; Zhao et al., 2011; Liu et al., 2015; Singha et al., 2016; De Bernardis et al., 2016; Liu et al., 2017; Zhao et al., 2018], showing different effects at various stages of development. The use, therefore, of the phenological information allowed by the availability of RS data allows to identify any morpho-physiological stresses during the life cycle of the vegetation.

Starting from these assumptions, the main objectives of this work were:

a) reconstructing the phenological trend of vegetation through NDVI in areas surrounding potentially polluted sites, on concentric areas at variable distances from the potential source of pollution. The aim was to verify the existence of variations in the functional parameters of the vegetation as you move away from the source of the contamination;
b) to compare the NDVI values of the vegetation, as a function of phenology, between the areas surrounding the sites with areas of the same vegetation typology, very distant from those potentially contaminated.

The comparison of physiological parameters, detectable through NDVI, between areas close to the sites and areas very distant concerning the possible influence of contaminants but in similar ecological conditions (climatic and pedological), allowed us to evaluate statistically the existence or not of alterations of the vegetation near the sites due to the contaminants during the phenological cycle.

2. Materials and methods

2.1 Study sites

The study areas for identifying the phenological trends of the vegetation consist of areas surrounding sites reported by the Basilicata Region as "potentially polluted". Such areas, currently abandoned and in the process of reclamation and restoration, have hosted municipal solid waste disposal activities over the years, starting in the early 1990s. The three study sites (for an exhaustive description of which see Mancino et al., 2022) are located in the north-western part of Basilicata (Figure 1), in the municipalities of Potenza (sites of Montegrosso-Pallareta and Vallone Calabrese) and of the neighboring municipality of Tito (site of Aia dei Monaci), respectively. The three sites share the fact that, in some phases of their management cycle, values of the monitored analytes were recorded above the threshold allowed by current legislation. In particular, the chemical elements out of range in some of the matrices analyzed (groundwater, surface water, soil) consisted of inorganic elements, especially iron, aluminum, nickel, lead, and selenium. The complex located in Aia dei Monaci (Tito) was first used as a landfill for municipal solid waste (MSW) from 1994 to 2004, when the authorized volumes were exhausted, and then as a waste transfer station for MSW, from 2007 to 2014. On the site of Montegrosso-Pallareta (Potenza), there is a complex of landfills whose work began in 1986 and that was responsible for waste disposal in May 1989. Since February 2009, it has housed an MSW transfer station inside of it. Nowadays, the activities of the waste transfer station are suspended. The former incinerator in Vallone Calabrese (Potenza), built between 1988 and 2003, only came into partial operation

at the end of 2005 with the start of the testing procedures, the “hot tests” of the industrial plants, pending the completion of the authorization process for the exercise. Up to that moment, the activity was provisional and never fully operational, which ended in 2007.

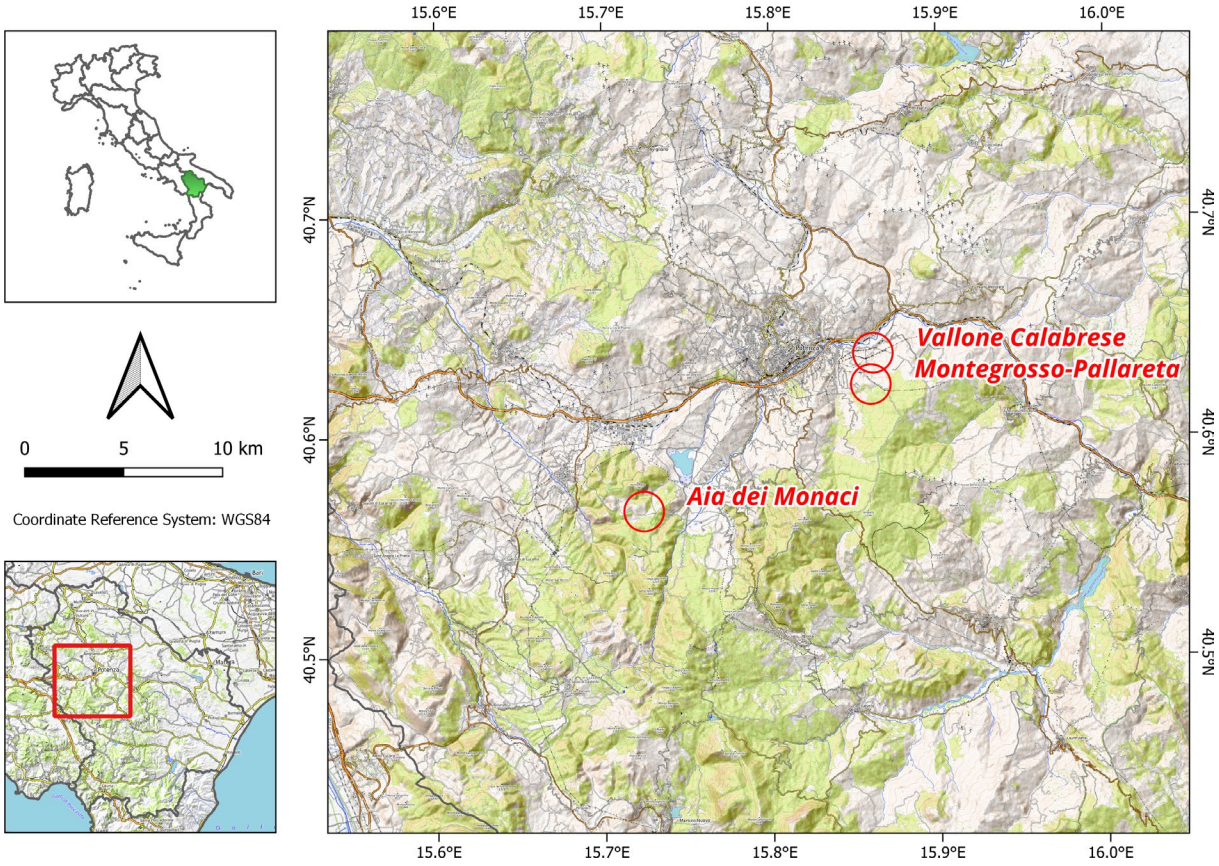


Figure 1. Overview of the study areas. Map data: OpenStreetMap contributors, SRTM | Map style: OpenTopoMap (CC-BY-SA) accessed on 17 March 2022.

2.2 Satellite data

To reconstruct the vegetation phenology of the areas adjacent to the study sites, the RS images of the Copernicus programme were used, in particular Sentinel-2 data, which have the advantage (Table 1) of a fine geometric resolution in the visible and near-infrared ranges. Furthermore, the relatively high revisitation frequency (approx. 2-3 days) generally allows a good time series to be available. The high repetitiveness, which results in 2-3 days at mid-latitudes, of the Copernicus Sentinel-2 mission is because it comprises a constellation of two polar-orbiting satellites (Sentinel-2 A e Sentinel-2 B, launched on June 22, 2015, and March 7, 2017, respectively) placed in the same sun-synchronous orbit, phased at 180° to each other.

The chosen survey year is 2017, therefore the images were identified that, in the various months, were of good quality and did not have cloud cover on the study areas. Due to the presence of cloud cover and poor image quality throughout the year, it was decided to identify one image per month (Table 2), all of which, however, were able to reconstruct the phenological trend of the various land use classes.

For some months (January, May, July, and November) it was not possible to identify quality images for the study areas as they all have very high cloud cover affecting these areas. Through the images selected, however, we were able to reconstruct the phenology of the vegetation types.

Sentinel-2 Level-1C, a Top-of-atmosphere reflectances (TOA) product, was downloaded, which was subsequently cloud-removed and atmospherically corrected, to obtain a Surface reflectance product (Level-2A). To remove the clouds from the Sentinel-2 scene, the IdePix (Identification of Pixels) algorithm was used, contained within ESA’s

Sentinel-2 Bands	Central Wavelength (µm)	Resolution (m)
Band 1 – Coastal aerosol	0.443	60
Band 2 – Blue	0.490	10
Band 3 – Green	0.560	10
Band 4 – Red	0.665	10
Band 5 – Vegetation Red Edge	0.705	20
Band 6 – Vegetation Red Edge	0.740	20
Band 7 – Vegetation Red Edge	0.783	20
Band 8 – NIR	0.842	10
Band 8A – Vegetation Red Edge	0.865	20
Band 9 – Water vapour	0.945	60
Band 10 – SWIR – Cirrus	1.375	60
Band 11 – SWIR	1.610	20
Band 12 – SWIR	2.190	20

Table 1. Geometric and radiometric characteristics of Sentinel-2 images.

Year	Month	Date of acquisition
2017	February	17/02/2017
2017	March	29/03/2017
2017	April	08/04/2017
2017	June	07/06/2017
2017	August	06/08/2017
2017	September	15/09/2017
2017	October	05/10/2017
2017	December	24/12/2017

Table 2. Sentinel-2 images used for the time series.

Sentinel Application Platform (SNAP) data management software [Wevers et al., 2021]. Subsequently, the Sentinel-2 images have been corrected with the Sen2Cor algorithm [Müller-Wilm, 2016a and 2016b] available within the SNAP application that allows atmospheric correction starting from the Top-of-Atmosphere (TOA) to obtain Bottom-of-Atmosphere (BOA) images. The model is based on an atmospheric correction algorithm of satellite images based on a radiative transfer model and which also uses reflectance Lambert's law.

Finally, the tiles were cropped on the study area in such a way as to include all three sites of interest and create the layer stacking for the subsequent temporal analysis (Figure 2).

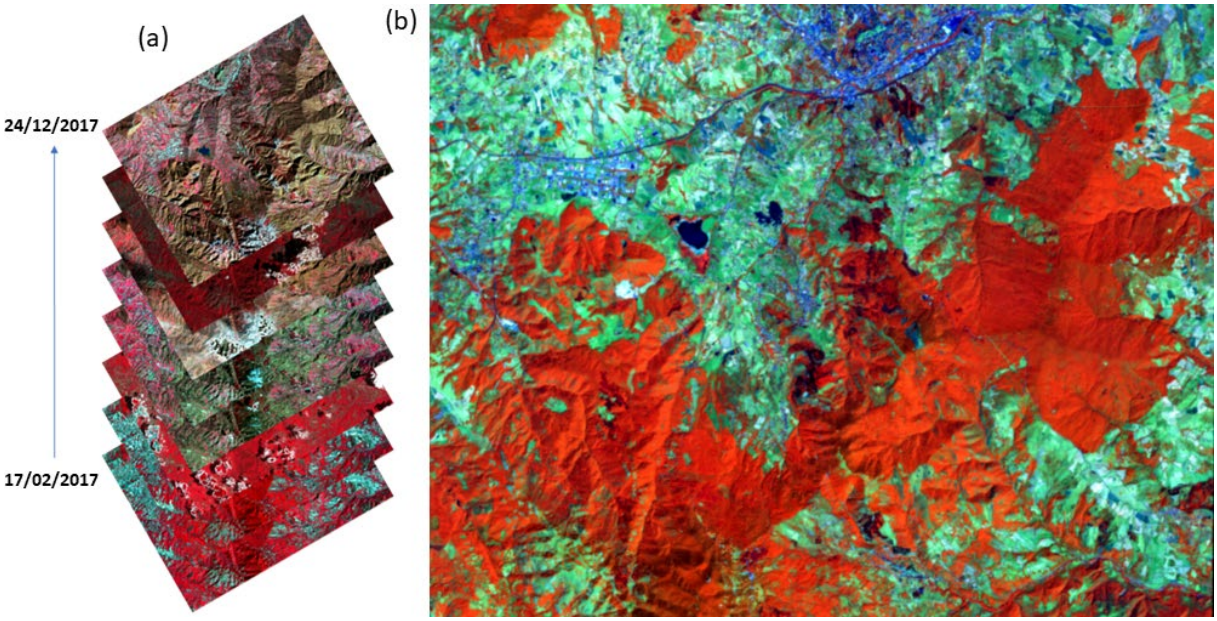


Figure 2. (a) Sentinel-2 layer stacking of the monthly images considered in the reconstruction of the vegetation phenology and (b) 8-11-2 band combination for the area of interest.

2.3 Analysis of phenology

For the analysis of the phenological trends of the vegetation and the spatial-temporal verification of any differences in the growth rates of the vegetation, a maximum area of 1 km radius was considered starting from the centroids of the various study sites, in consideration of the fact that physiological variations, in the various stages of growth, are evident in an area not far from potentially polluted sites [Atkinson and Curran, 1997; Huang et al., 2016; Mancino et al., 2022].

Centroid buffers of the site (Table 3) were considered at a distance gradually increasing in the hypothesis that the effect of contamination by PTEs is reduced by moving away from the potential source of pollution. The aim, therefore, was to verify the existence or not, for the different types of vegetation, of differences in the functional efficiency of the vegetation depending on the distance from the sites, considering the degradation that the pollutants undergo from the point of emission to the surrounding areas following the transport routes [McGwire et al., 1993; Li et al., 2021].

Once the concentric areas were identified, a total of 300 control points for each site were selected, adopting a random-stratified criterion (Figure 3). The stratification took place considering the surface of the different annulus and land use/land cover (LULC), selecting the sample size in proportion to the areas occupied by the different land use types. It is therefore a stratified random sampling, in which the stratum is represented by the land use present in the buffers. Also considering the spatial resolution of the Sentinel-2 bands used (10 m), a minimum distance between the points of 15 m was set so that only one point could fall within one pixel.

For each sample point, the corresponding land use was identified using the Land Use map of the Basilicata Region and verifying its correctness through the visual analysis of the 2017 AGEA orthophoto. Finally, for the various sets of points grouped by land use classes, the mean NDVI value was extracted for the available months of Sentinel-2 images.

Buffer	Internal radius (m)	External radius (m)
1	0	200
2	200	350
3	350	500
4	500	1000

Table 3. Buffer adopted in the analysis of phenological trends. The internal and external radius refers to the centroid of the site.

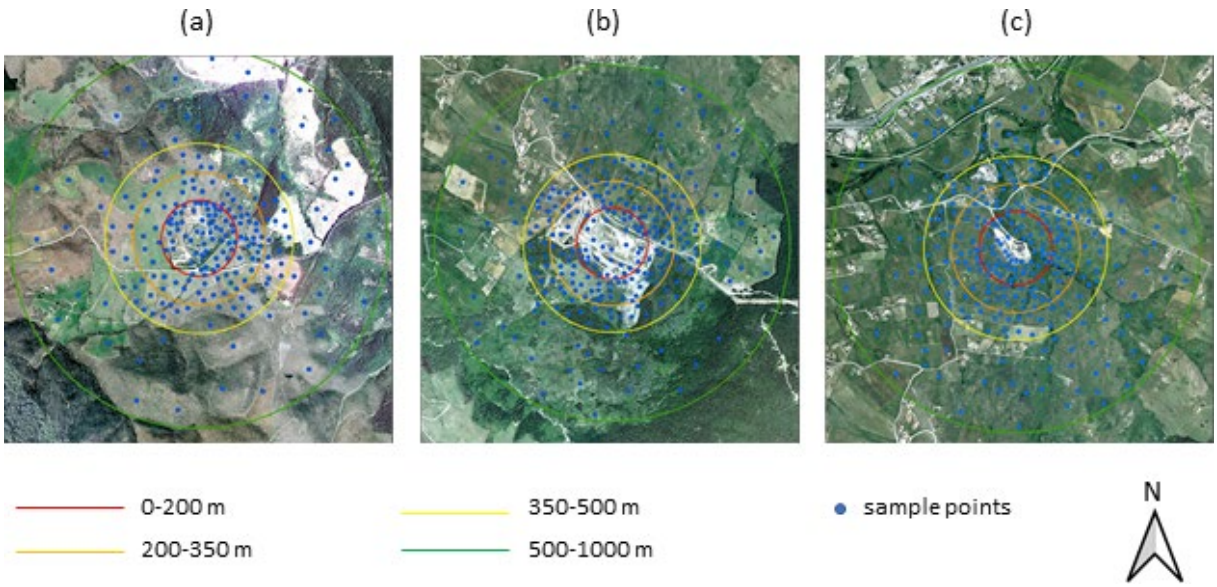


Figure 3. Sample points selected in concentric buffers for: (a) Aia dei Monaci, (b) Montegrosso-Pallareta, and (c)Vallone Calabrese.

The phenology was analyzed both on the entire area (radius of 1 km from the site's centroid) and, separately, for the four buffers to verify the existence of significant differences in the physiological efficiency of the vegetation as we move away from the potential source of pollution. For the analysis of phenology, the NDVI index was used, given by the normalized difference of the red and NIR bands and which for Sentinel 2 images takes the following formulation (Eq. 1):

$$NDVI = \frac{band\ 8 - band\ 4}{band\ 8 + band\ 4} \quad (1)$$

NDVI is certainly the best-known and tested Vegetation Index (VI) and can identify the amount of biomass in plant formations [Yoder and Waring; 1994; Goetz and Prince, 1996; Myneni et al., 1997; Mancino et al., 2020] and morphological and functional variations, such as chlorophyll content, photosynthetic activity, leaf area index, chlorosis, crown transparency, etc. [Pettorelli et al., 2005; Li et al., 2014; Liu et al., 2015; Liu et al., 2016; Jin et al., 2017] induced by HM contamination. NDVI is able to express the physiological stresses of vegetation during the various phases of its development [Daughtry et al., 2000; Pettorelli et al., 2005; Glenn et al., 2008; Jiang et al., 2017; Bachmair et al., 2018; Kang et al., 2021; Hu et al., 2021].

Even in the hypothesis that the points detected in the buffer at a greater distance from the potential source of pollution could be considered points potentially not subject to contamination, to further corroborate the thesis, control points have been identified in areas very distant from the sites. Such points, selected within the whole considered spatial extent, fall into areas in similar conditions from an ecological point of view (altitude, slope, climatic parameters, etc.) concerning the areas adjacent to the sites of interest. The distance from the sites, and therefore the absolute impossibility of representing a target of potential contamination, makes these points considered as unpolluted reference points (URPs). For the selection of the URPs, the land use present both in the areas bordering the study sites (in the 1 km buffer) and throughout the entire survey area was taken into account (fig 2b). The area is mainly occupied (over 50%) by Broad-leaved forests (code 311) and by Non-irrigated arable land (code 211) for approx. 20%. Follow, in order of extension, Transitional woodland/shrub (code 324) which covers an area of approx. 12% and Natural grassland (code 321) for over 7%. Of lesser importance, in terms of extension, are Coniferous forests (312) and Permanently irrigated land (code 212), each of which covers an area of 2-3%. The unpolluted reference points were selected in an almost proportional way to the areas of various land use types, selecting a total of 95 points.

The seasonal trends of NDVI were therefore compared, considering all the points falling within the 1 km buffer, stratified by land use, with the phenology of the URPs belonging to the corresponding land use classes.

To verify the significance of the difference in phenological trends between URPs and areas contiguous to the sites, a statistical analysis was carried out using indices able to measure the dissimilarity between time series [Esling & Agon,2012; Wang et al., 2012]. Specifically, Euclidean Distance (ED), Cross correlation based distance (ccor), Short time series distance (STS), and Autocorrelation-based Dissimilarity (ACF) were used.

ED (Eq. 2) computes the Euclidean distance between a pair of numeric vectors of the same length:

$$D = \sum \sqrt{(x_i - y_i)^2} \tag{2}$$

where:
x = numeric vector containing the first time series.
y = numeric vector containing the second time series.

Cross correlation based distance computes the distance measure based on the cross-correlation between a pair of numeric time series [Liao, 2005; Pree et al., 2014].

The cross-correlation (Eq. 3) based distance between two numeric time series is calculated as follows:

$$D = \sqrt{\frac{1-CC(x,y,0)^2}{\sum_{k=1}^{lag.max}(1-CC(x,y,k)^2)}} \tag{3}$$

where $CC(x, y, k)$ is the cross-correlation between x and y at lag k.

The summatory in the denominator goes from 1 to lag.max. Given this, the parameter must be a positive integer not larger than the length of the series.

Short time series distance (STS) computes the short time series distance between a pair of numeric time series. STS is designed especially for series with an equal but uneven sampling rate [Möller-Levet et al., 2003]. However, it can also be used for time series with a constant sampling rate. It is calculated as follows (Eq. 4):

$$STS = \sum_{k=1}^{1-N} \left(\frac{y_{k+1}-y_k}{tx_{k+1}-tx_k} - \frac{x_{k+1}-x_k}{ty_{k+1}-ty_k}\right)^2 \tag{4}$$

where
x Numeric vector containing the first time series.
y Numeric vector containing the second time series.
tx If not constant, a numeric vector that specifies the sampling index of series x.

ty If not constant, a numeric vector that specifies the sampling index of series y.
N is the length of series x and y and the summatory goes from 1 to one minus the length of the series.
tx and ty must be positive and strictly increasing. Furthermore, the sampling rate in both indexes must be equal:

$$tx[k+1] - tx[k] = ty[k+1] - ty[k], for\ k = 0, \dots, N-1$$

Autocorrelation-based Dissimilarity (ACF) computes the dissimilarity between a pair of numeric time series based on their estimated autocorrelation coefficients [Galeano and Pella, 2000].

The Autocorrelation-based Dissimilarity index [Galeano and Peña, 2000; Lei and Sun, 2007; Diaz and Vilar, 2010; Montero and Vilar, 2014] calculates a dissimilarity measure between two-time series based on their estimated autocorrelation functions (ACF) to consider the dependence structure of time series. More in detail, considering uniform weights, it is calculated as the Euclidean distance between ACF (Eq. 5):

$$d(X,Y) = \sqrt{\sum_{r=1}^{R}\left(\rho_{X,r} - \rho_{Y,r}\right)^2} \quad (5)$$

where ρ_X and ρ_Y are respectively the estimated autocorrelation vectors of the time series X and Y for some R such that $\rho_{Xi} \approx 0$ and $\rho_{Yi} \approx 0$ for $i < R$. $r = 1, \dots, R$ refers to lag of X and Y time series.

3. Results

The phenological trend for the year 2017 was therefore reconstructed for the various types of land use falling within the three areas of interest. Such trends are subdivided according to the distance from the centroid of the potentially polluting site (Figure 4).

For Aia dei Monaci (Figure 4a), the trend of "Arable land in non-irrigated areas", basically attributable to wheat and secondarily or to other cereals (as shown by digital datasets on the RSDI Basilicata Region geoportal), evaluated on the entire study area is the expected one and follows the phenology of such species in the Mediterranean climate. The phenological trend, for the different buffers, shows a very limited variability, probably due to the absence of variations as a function of the distance from the potentially polluting area. The seasonal trends are almost overlapping but also the differences for the different dates are very limited and attributable, where they exist, to different local fertility conditions (altitude, exposure, soil characteristics).

For the "Broad-leaved forest", both the trends and the NDVI values achieved in the various months are in line with those expected and no significant differences are highlighted. The only exception is represented by buffer 1, in which the mean NDVI values are strongly below the values recorded in the other buffers. What might seem an anomaly resulting from a problem of eco-physiological efficiency, is instead due to differences in the plant species involved, as better described in the next paragraph.

Even the "Natural grasslands" in Aia dei Monaci, attributable to the grazing areas, present in buffers 1, 2, and 4 do not show anomalous trends that can be attributed to the effect of potential pollution. The phenological trends are those expected with higher NDVI values in the autumn and spring months and with a strong reduction in the summer months. Among other things, the NDVI values of the pasture areas of the 1st buffer are generally more sustained than the buffers further away from the site, demonstrating the non-existence of vegetation stress due to the landfill activity. The "Transitional woodland-shrub" consists of generally sparse tree stands in which the shrub component plays a fundamental role in terms of abundance/dominance. This is evidenced by the trends of NDVI over the years, more similar to pastures and tree pastures than to proper forests. The considerable variability both in terms of species composition and density leads to a certain variability within the buffers but is attributable to natural effects. Buffer 1 has higher values in the autumn-winter and spring months as evidence that the spatial variations in terms of NDVI are due to the typology or structure of these stands.

For the Montegrosso-Pallareta site, the phenological trends of the different land use and for the different buffers are shown in Figure 4b. The "Non-irrigated arable land" does not have significant spatial differences such as being

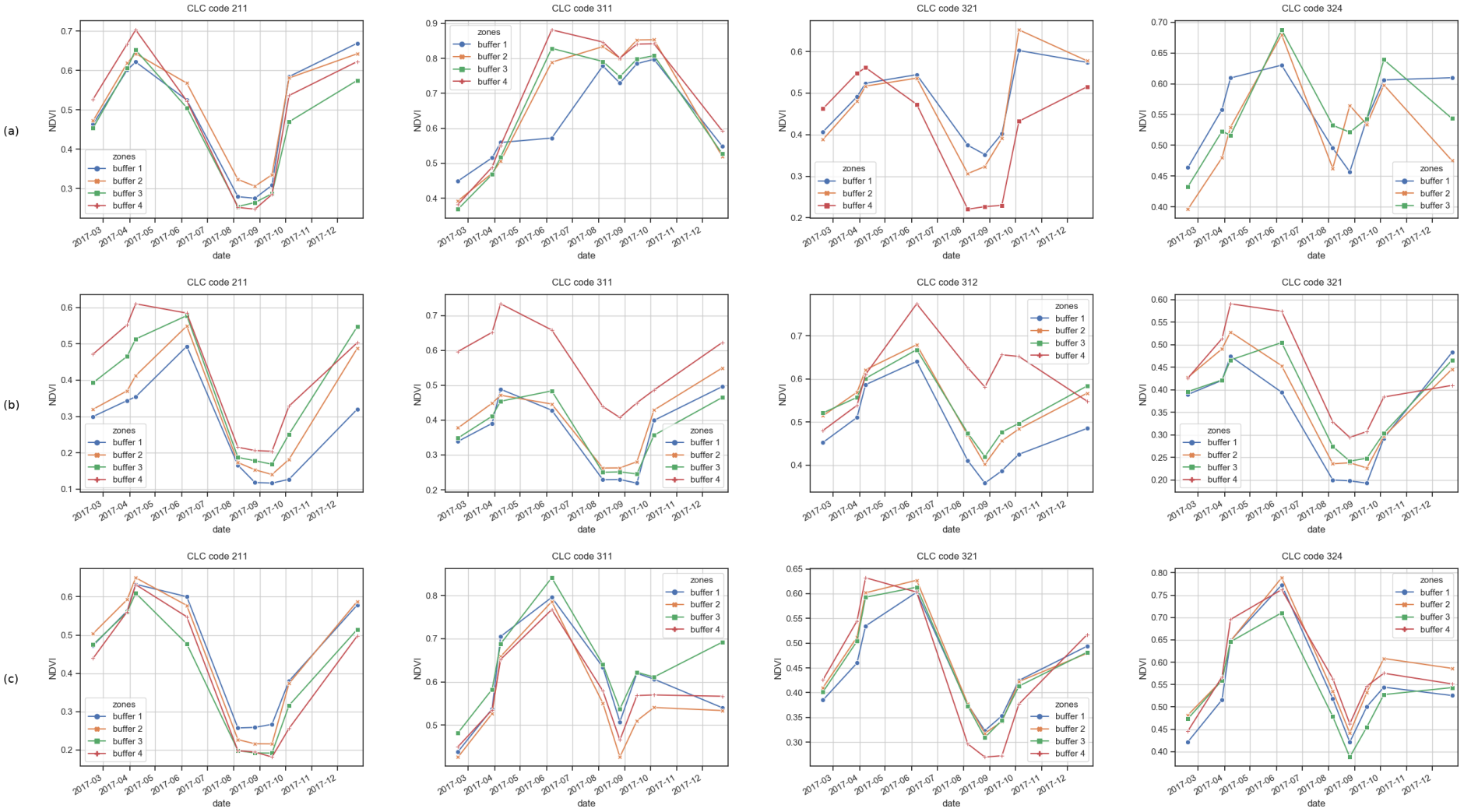


Figure 4. Phenological trends of different land use classes, subdivided by buffer, for the considered case studies: (a) Aia dei Monaci, (b) Montegrosso-Pallareta and (c) Vallone Calabrese (class description: 211—Non-irrigated arable land, 311—Broad-leaved forest, 312—Coniferous forest, 321—Natural grasslands, 324—Transitional woodland-shrub).

able to trace these to potential effects of pollution. The NDVI increases with increasing distance from the site but the effect is attributable to local characteristics. By crossing the data, in fact, with the morphological layers (altitude, slope, and aspect) it clearly denotes how as you move away from the site, the altitudes and slopes tend to decrease, as well as the aspect (in the southern quadrants) they are more favorable to the crop species which registers, in these conditions, higher productivity values. For the "Broad-leaved forest," there is a perfect agreement on both the trends and NDVI values, between the different buffers, in particular buffers 1, 2, and 3. Only buffer 4 has the same trend but significantly higher values. Moreover, as better specified in the discussions, the differences between trends are due to the presence of different tree species with various levels of productivity.

A similar argument concerns the "Coniferous forest", namely reforestations realized in different years (and therefore with a different stage of development) around this study site. The forest fire mentioned above mainly affected the reforestation of conifers present in buffers 1, 2, and 3, causing an abrupt decrease of the NDVI values, while it did not affect the reforestation present in buffer 4. This justifies the close analogy of the trends and values of NDVI in the first three buffers and of the difference with the values and in the trends of buffer 4. The wildfire occurred on 21 and 22 July 2015, and affected a large area, approx. 60 ha, involving the area to the south and east of the landfill. It was a high intensity fire that required the intervention of aircraft for its extinguishing. It involved both grasslands and scrubby pastures and a considerable part of the coniferous forests, mainly *Pinus halepensis*, in the areas closest to the landfill.

For the "Natural grasslands", the situation is similar to that of the Aia dei Monaci site and the "Non-irrigated arable land" of this same site: the differences, not statistically significant, are due to the type of pasture and the quantity of biomass present in relation to the local conditions. The pastures in better conditions, and therefore with higher NDVI values, are present in buffer 4, where there are lower altitude and slope values than the other buffers.

The "Non-irrigated arable land" in Vallone Calabrese (Fig. 4c) does not present significant spatial differences. The values and trends are almost similar. Buffer 1 even records values that are always higher than the other buffers, as evidence of the non-existence of a vegetational stress effect as a result of anthropogenic activity in the study site.

Also for the "Broad-leaved forest" and the "Transitional woodland-shrub" there are no significant spatial patterns. The slight differences between the different buffers are simply due to the different types of species present in the different areas. Oak forests always have higher NDVI values than chestnut groves (although the differences are limited) and both with values, as found in other sites, significantly higher than in the "Other broad-leaved" category.

To further corroborate this conclusion, the analysis of NDVI seasonal values and trends for the different land use categories was also conducted on points very distant from the sites of interest (Figure 5). Basically, the average values of the VI were compared considering all the pixels of the entire area of the three sites (falling within the 1 km buffer), stratified by land use, with other areas, very distant from the sites but in similar ecological conditions (altitude, slope, pedology, climate, etc.). These points can be considered as URPs, i.e. areas where the potential effect of the pollutants introduced into the environment by the specific activities of the three sites is not affected in any way.

To verify the significance of the difference in phenological trends, some statistical indicators of dissimilarity of the time series were used (Table 4). The statistical indicators of dissimilarity used in the analysis are expressed in terms of distance between two-time series, thus they potentially range from 0 to infinite. A high indicator value indicates a great level of dissimilarity between the time series being compared, while 0 indicates perfect similarity/correlation.

For the Aia dei Monaci site, the comparison between the phenological trends of land uses included within the 1 km buffer and the URPs is shown in Figure 6.

The trends show that, for all land use classes, there is no substantial difference between the areas within the study site and the URPs of the same categories selected in a large area outside the potential effect of pollutants. For all land uses, even the average NDVI values for the various months reach slightly higher values at the Aia dei Monaci site, further confirming the non-existence of vegetation stress in the areas bordering the site of the former Tito landfill.

The statistical analysis of trend dissimilarities confirms the concordance of phenological trends between the areas bordering the sites and those of the areas very distant from them (URPs): all the indices used, in particular ED and ccor, show a greater concordance for "Broad-leaved forest" and "Natural grasslands", although also the trends of "Non-irrigated arable land" and "Transitional woodland-shrub" do not show significantly different phenological trends. For the Montegrosso-Pallareta site (Figure 7), the phenological trends between the white areas and those near the sites do not show significant differences both in terms of "Non-irrigated arable land" and "Natural grasslands". Significant differences, on the other hand, are noted for the forest areas, both the "Broad-leaved forest" and the "Coniferous forest". These differences, however, as previously mentioned, and as will be discussed later, are unequivocally due to external factors with respect to PTEs pollution.

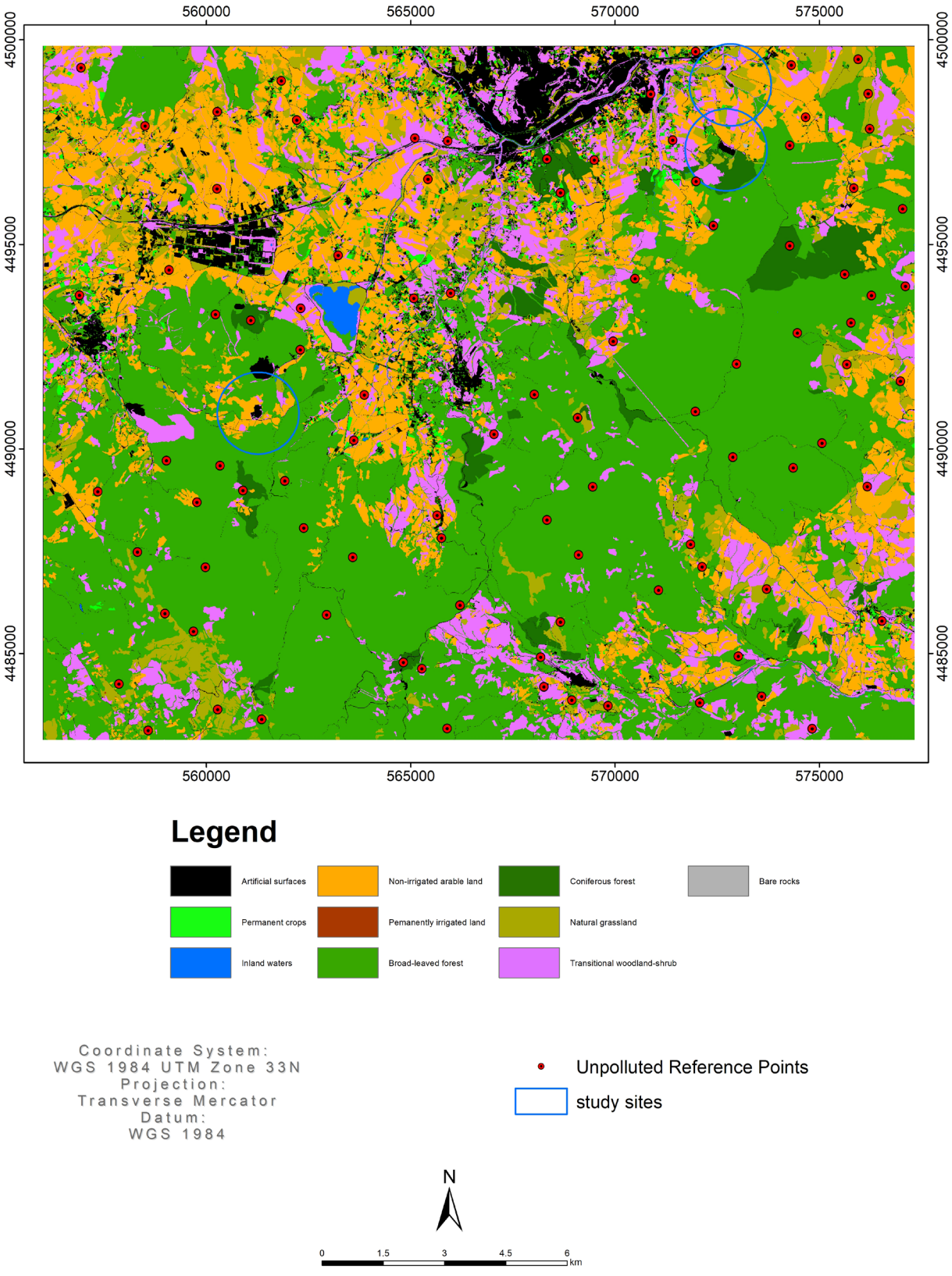


Figure 5. Land use map and URP identification.

Aia dei Monaci

Land use	Land use class code	ED	ccor	STS	ACF
Non-irrigated arable land	211	0.288	0.524	0.156	0.416
Broad-leaved forest	311	0.120	0.155	0.084	0.121
Natural grassland	321	0.164	0.474	0.099	0.095
Transitional woodland/shrub	324	0.130	0.632	0.062	0.298

Montegrosso-Pallareta

Land use	Land use class code	ED	ccor	STS	ACF
Non-irrigated arable land	211	0.103	0.379	0.083	0.241
Broad-leaved forest	311	0.439	0.878	0.168	0.760
Coniferous forest	312	0.293	0.786	0.076	0.468
Natural grassland	321	0.131	0.493	0.065	0.340

Vallone Calabrese

Land use	Land use class code	ED	ccor	STS	ACF
Non-irrigated arable land	211	0.194	0.431	0.132	0.176
Permanently irrigated land	212	0.352	0.621	0.196	0.500
Broad-leaved forest	311	0.609	1.433	0.250	1.006
Natural grassland	321	0.201	0.792	0.154	0.388

Table 4. Dissimilarity indices for each study site and for different land use classes.

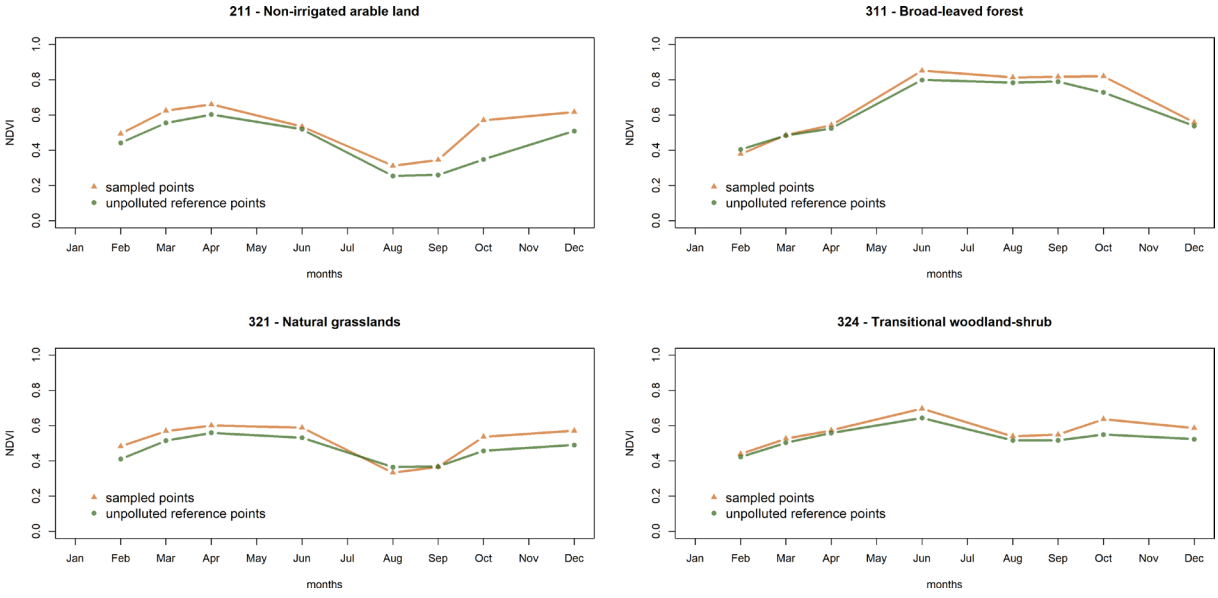


Figure 6. Comparison between the phenological trends of various land use classes, in areas near Aia dei Monaci and the URPs.

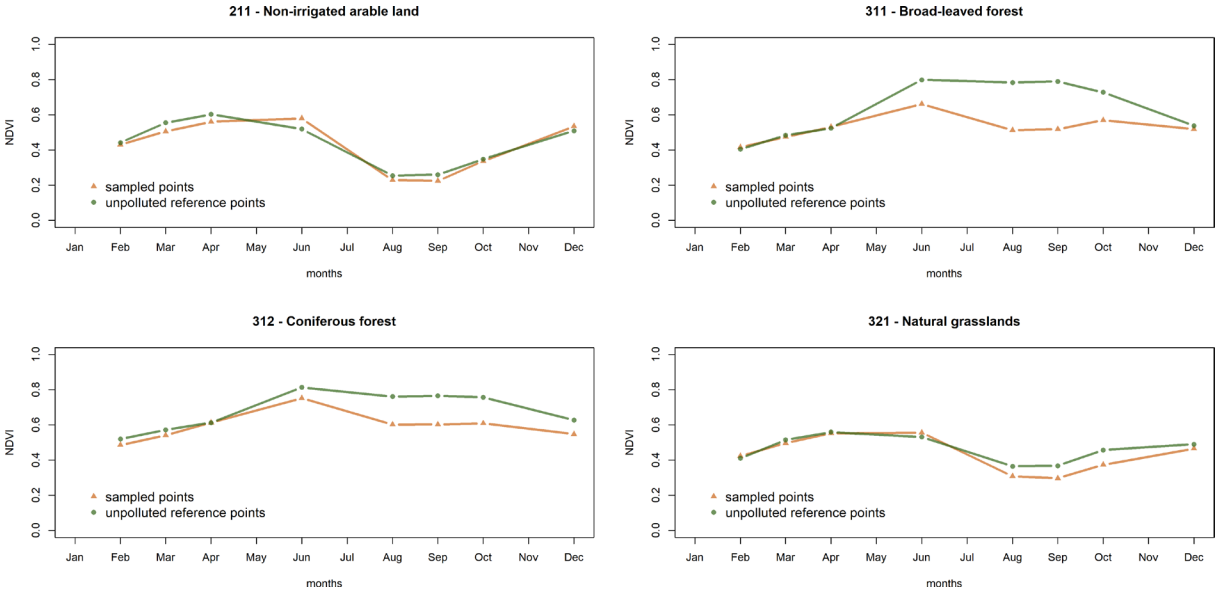


Figure 7. Comparison between the phenological trends, for the various land uses, of the areas bordering the Montegrosso-Pallareta site and the URPs.

All statistical indices of dissimilarity confirm that "Non-irrigated arable land" is the land use class that shows greater agreement in phenological trends, followed by "Natural grasslands". Both broad-leaved and coniferous forest, on the other hand, show significantly different trends. The indices, with the exception of STS which proved to be the least performing index in all situations, show higher dissimilarity for "Broad-leaved forest", followed by "Coniferous forest". For the site of the former incinerator of Vallone Calabrese, the comparison with the URPs is shown in Figure 8. Also in this case there are no substantial differences in phenological trends, especially for "Non-irrigated arable land", while the "Irrigated arable land" near the site show NDVI values that tend to be higher than the URPs.

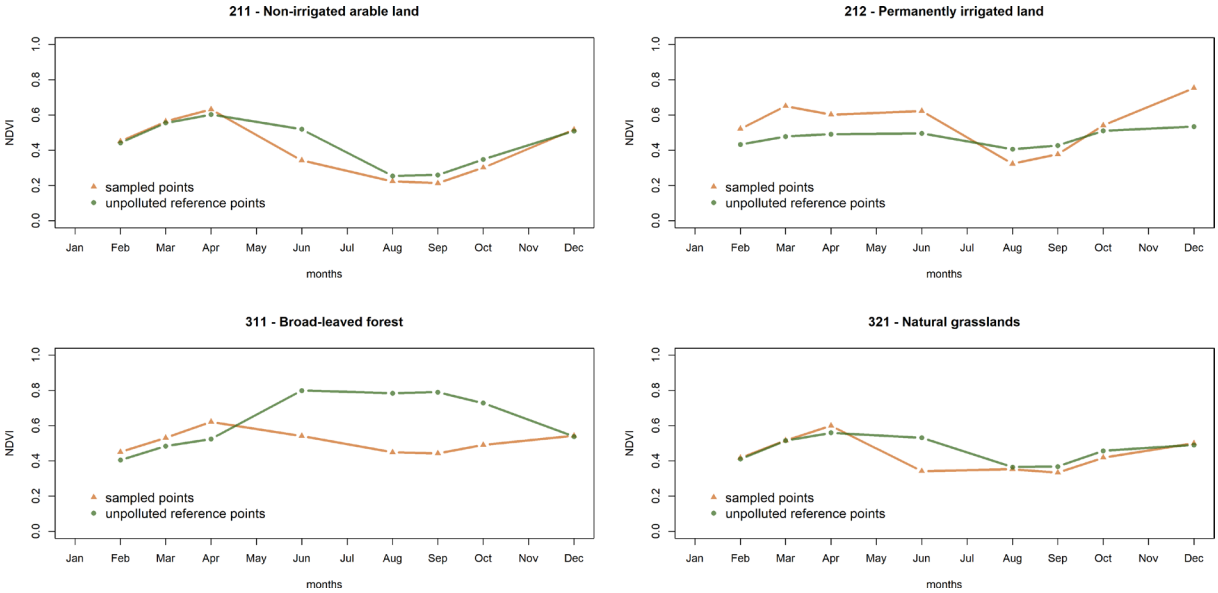


Figure 8. Comparison between the phenological trends, for the various land uses, of the areas bordering the Vallone Calabrese site and the URPs.

The statistical indices of dissimilarity (Table 4) confirm that the phenological trends of non-irrigated arable crops show the highest agreement among land uses types. The trends relating to "Natural grasslands'' also show statistically insignificant differences due to the different density attributable to the different fraction of the shrub component, as highlighted by the visual analysis of the AGEA 2017 orthophotos.

Instead, very marked differences, statistically significant, are recorded for the phenological trends relating to the "Broad-leaved forest", to be traced back, however, to the different types of forest stands which have very dissimilar density values, as will be discussed later.

4. Discussions

For the broad-leaved forests in Aia dei Monaci, both the trends and the NDVI values achieved in the various months are consistent with those expected and there are no significant differences. The only exception is represented by buffer 1, in which the average NDVI values for broad-leaved forest (Fig. 4a) are strongly below the values recorded in the other buffers. What might seem an anomaly to be traced back perhaps to a problem of eco-physiological efficiency is instead due to the type of tree vegetation present in this buffer. Broad-leaved forests are, in fact, a broad category of possible forest types, very different from a compositional and structural point of view, therefore the hypothesis was that the differences could be due not to the potential effects of pollution but to a compositional, structural, and functional biodiversity that affects the reflectance characteristics.

The intersection between the buffers and the fourth level Land Use map, which specifies the different forest types, highlights how the "Other mesophilous and meso-thermophilous broad-leaved forests" (3113 class code) fall into buffer 1, while the broad-leaved forest attributable to the other buffers are attributable to "Deciduous oak forests" (3112 class code). Class 3113 (Figure 9) essentially consists of shrub and tree stands with decidedly lower density values than oak forests and which therefore have lower NDVI values, especially during the growing season.

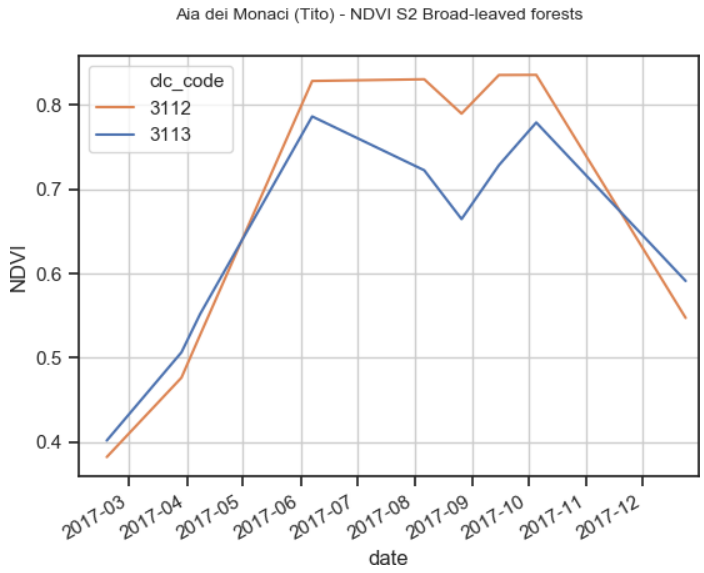


Figure 9. Phenological trend of broad-leaved forests classes for the Aia dei Monaci site.

For the Montegrosso-Pallareta site, for the "Broad-leaved forest" (Fig. 4b) there is a perfect agreement on the trends, and the NDVI values, between the different buffers, especially between buffers 1, 2, and 3. Only buffer 4 shows the same trend but significantly higher values. This is essentially due to two factors: the fire that occurred in July 2015 which affected part of the broad-leaved forest of buffers 1, 2 and 3 and which therefore caused a significant decrease of the NDVI values and the presence, in buffer 4, of a different type of deciduous trees. In particular, while in buffers 1, 2, and 3 there are "Other mesophilous and meso-thermophilous broad-leaved forests" (3113), in buffer 4 there are mainly stands attributable to "Deciduous oak forests". The latter have significantly higher NDVI values

than the mesophilous broadleaves, which are, in the case in question, due to thermophilous shrubs and riparian vegetation.

The analysis becomes even more explicit by comparing the broad-leaved forest, disaggregated into subclasses 3112 ("Deciduous oak forests") and 3113 ("Other mesophilous and meso-thermophilous broad-leaved forests"), falling into the buffer at 1 km with those of the URPs (Figure 10).

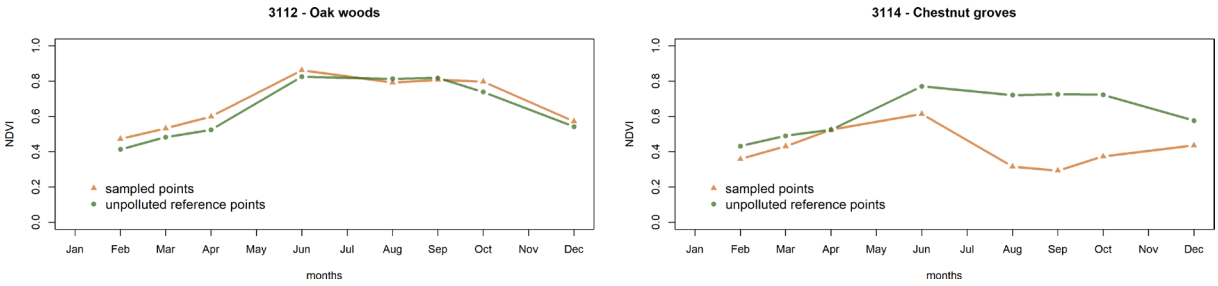


Figure 10. Comparison between the phenological trends of broad-leaved forests classes between the areas bordering the site of Montegrosso-Pallareta and the URPs.

The substantial differences, which are denoted by class 311 (Broad-leaved forest), are due to the presence in the areas close to the Montegrosso-Pallareta site of "Chestnut groves" (code 3114). These are chestnut coppices subjected to forest harvesting, as the photo-interpretation of the AGEA 2017 orthophoto has allowed us to ascertain, which caused a sharp lowering of the NDVI values as a result of the cutting down trees. Comparing only the "Deciduous oak forests" class (code 3112), it is possible to verify that there are no substantial differences between the stands near the site and those very far from it.

Even in the case of the Montegrosso-Pallareta site, there are no anomalies on the vegetation trends, such that they can be traced back to eco-physiological stress as a result of pollution phenomena.

For Vallone Calabrese, there are no significant spatial patterns for the "Broad-leaved forest". The slight differences between the different buffers are simply due to the different types of species present in the different buffer areas. Oak forests always have higher NDVI values than chestnut groves (although the differences are limited) and both with values, as found in the other sites, significantly higher than the category "Other mesophilous and meso-thermophilous broad-leaved forests". The latter, in fact, show high variability in terms of tree cover: within the buffer at 1 km of the site, these stands have poor coverage values and therefore significantly lower NDVI values than the URPs (Figure 11).

Furthermore, the decrease of the NDVI values of the "Broad-leaved forest" class is due to the contribution of the "Chestnut groves" subclass within the site (Fig.11). The latter shows a sharp drop in NDVI values after the month of June due to a tree cut, as evidenced by both the time-series analysis and the visual interpretation of the 2017 orthophotos.

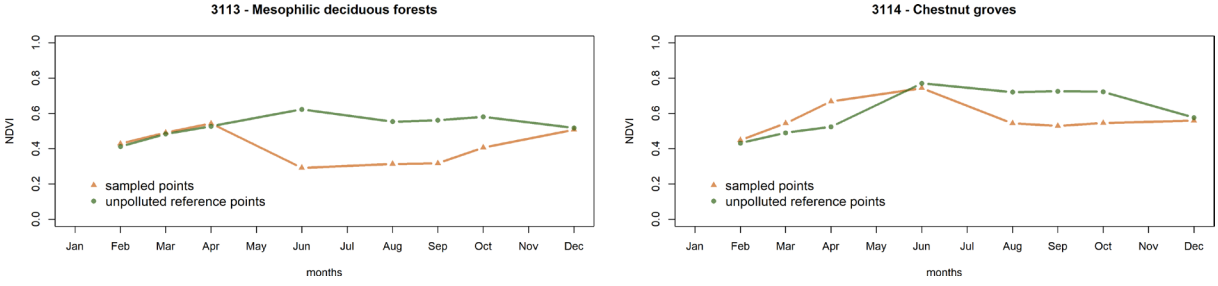


Figure 11. Comparison between the phenological trends of broad-leaved forests near the Vallone-Calabrese site and in URPs.

5. Conclusions

The analysis of the spatial differences of the vegetation trends relating to the year 2017, for the three study sites, does not show significant differences as the distance from the site increases. The starting hypothesis is that the effect on the vegetation of any pollution due to PTEs reduces with the distance from the potential pollutant source. Furthermore, the comparison between the phenological trends of the areas near the potentially polluting sites and those of the same land uses, in similar ecological conditions, but very far from the sites and therefore such as to be considered URPs, does not show any substantial differences, statistically significant, in term of seasonal growth rates.

The adopted methodology allows to identification the presence or absence, relative to the year of interest, of stress induced on the vegetation, correlated with the waste disposal activities, such as to affect the physiological efficiency of the vegetation and, therefore, on functional alterations of the same.

Thus, the time-series analysis of phenological trends of vegetation could be applied to the numerous sites (almost 400) reported as "potentially polluted" by the Basilicata Region (http://rsdi.regione.basilicata.it/geoserver/www/bonifica/index.html) to verify the existence of degradation processes of the natural ecosystems surrounding these sites. The usefulness of such an approach consists of the fact that a cost-effective decision support tool is available that can be used in an initial evaluation/screening phase of the sites to be subjected to environmental remediation.

Ultimately, such a methodology implemented in this work can be generalized and exported to other territorial contexts and for any other anthropic activity or natural event that is believed to represent, both locally and on a large scale, a stressor such as to affect the functional efficiency of the vegetation. For this purpose, it could be interesting to compare, using the methodological procedure of the present study, the phenological trends elaborated with NDVI and those elaborated using other Vegetation Indices, particularly suitable for identifying vegetation stress. In particular, it could be interesting to test, in comparison to NDVI, the significance of indices capable of analyzing phenology (e.g.: NDPI, Normalized difference phenology index), the water content of the canopy (e.g.: NDWI, Normalized difference water index), the amount of non-photosynthesizing biomass compared to the amount of total biomass (e.g.: NDTI, Normalized difference tillage index), or the chlorophyll content (e.g.: S2REP, Sentinel-2 Red-Edge Position Index; IRECI, Inverted Red-Edge Chlorophyll Index, etc.). Finally, the analysis of the phenological trends elaborated on longer historical series could provide more robust results, as the variations of NDVI due to meteorological fluctuations would be taken into greater consideration.

Acknowledgments. We sincerely thank the anonymous reviewers for the useful suggestions on improving the quality of the manuscript. The present work was a further result of the project "SIMBioSi" (2017-2019), co-financed by the Basilicata Region. The APC was funded by Centro di Geomorfologia Integrata per l'Area del Mediterraneo.

Data Availability Statement. The data presented in this study are openly available here: http://www.webgis-simbiosi.it/

References

Arun, K.S., C. Cervantes, H. Loza-Tavera and S. Avudainayagam (2005). Chromium toxicity in plants, Environ. Int., 31, 739-753.

Atkinson, P.M. and P.J. Curran (1997). Choosing an appropriate spatial resolution for remote sensing investigations, Photogramm. Eng. Remote Sens., 63, 1345-1351.

Austruy, A., N. Wanat, C. Moussard, P. Vernay, E. Joussein, G. Ledoigt and A. Hitmi (2013). Physiological impacts of soil pollution and arsenic uptake in three plant species: *Agrostis capillaris*, *Solanum nigrum* and *Vicia faba*, Ecotoxicol Environ. Saf., 90, 28-34.

Bachmair, S., M. Tanguy, J. Hannaford and K. Stahl (2018). How Well Do Meteorological Indicators Represent Agricultural and Forest Drought across Europe?, Environ. Res. Lett., 13, 034042.

Boularbah, A., C. Schwartz, G. Bitton and J.L. Morel (2006). Heavy metal contamination from mining sites in South Morocco: 1. Use of a biotest to assess metal toxicity of tailings and soils, Chemosphere, 63, 802-810.

Brimer, L. (2011). Chemical food safety. CABI (Editor), United Kingdom, 296.

Broge, N.H. and E. Leblanc (2001). Comparing Prediction Power and Stability of Broadband and Hyperspectral Vegetation Indices for Estimation of Green Leaf Area Index and Canopy Chlorophyll Density, Remote Sens. Environ., 76, 156-172.

Burton, K.W., E. Morgan, and A. Roig (1986). Interactive Effects of Cadmium, Copper and Nickel on the Growth of Sitka Spruce and Studies of Metal Uptake from Nutrient Solutions, The New Phytologist, 103, 3, 549-557.

Bussotti F. and M. Ferretti (1998). Air pollution, forest condition and forest decline in Southern Europe: an overview, Environ. Pollut., 101, 49-65.

Carlson R.W., F. A. Bazzaz and G. L. Rolfe (1975). The effect of heavy metals on plants: II. Net photosynthesis and transpiration of whole corn and sunflower plants treated with Pb, Cd, Ni, and Tl, Environ. Res., 10, 1, 113-120.

Chaplygin, V., T. Minkina, S. Mandzhieva, et al. (2018). The effect of technogenic emissions on the heavy metals accumulation by herbaceous plants, Environ Monit Assess, 190, 124.

Chatterjee, J. and C. Chatterjee (2000). Phytotoxicity of cobalt, chromium and copper in cauliflower, Environ. Pollut., 109, 1, 69-74

Chen, J., S. Shiyab, F.X. Han, D.L. Monts, C.A., Waggoner, Z. Yang, and Y. Su (2008). Bioaccumulation and Physiological Effects of Mercury in Pteris Vittata and Nephrolepis Exaltata, Ecotoxicology, 18, 110-121.

Cheng, S.P. (2003). Effects of heavy metals on plants and resistance mechanisms, Environ. Sci. Pollut. Res., 10, 256-264.

Chi, G., B. Huang, X. Chen, Y. Shi and T. Zheng (2011). Effects of Cadmium on Visible and Near-Infrared ReflectanceSpectra of Rice (*Oryza sativa* L.), Fresenius Environ. Bull., 20, 391-397.

Ciesla, W.M., E. Donaubauer and Food and Agriculture Organization of the United Nations. (1994). Decline and Dieback of Trees and Forests: A Global Overview, FAO Forestry Paper, 120, 90 pp.

Clauser, F. and R. Gellini (1986). Rating of Waldsterben symptoms (forest decline) in deciduous broadleaves during winter time, Eur. J. For. Path., 16, 250-253.

Choe, E., F. van der Meer, F. van Ruitenbeek, H.;van der Werff, B. de Smeth and K.-W. Kim (2008). Mapping of Heavy Metal Pollution in Stream Sediments Using Combined Geochemistry, Field Spectroscopy, and Hyperspectral Remote Sensing: A Case Study of the Rodalquilar Mining Area, SE Spain, Remote Sens. Environ., 112, 3222-3233.

Cowling, E.B. (1986). Regional declines of forest in Europe and North America: the possible role of airborne chemicals, in Aerosols. Research, risk, assessment and control strategies. (Editor) by S.D. Lee, T. Schneider, L.D. Grant, P.J. Verkerk. Lewis Oubl. Inc., Chelsea (USA), 855464.

Daughtry, C.S.T., C.L. Walthall, M.S. Kim E.B., de Colstoun, and J.E. McMurtrey (2000). Estimating corn leaf chlorophyll concentration from leaf and canopy reflectance, Remote Sens. Environ., 74, 229-239.

De Bernardis, C., F. Vicenteguijalba, T. Martinezmarin and J. Lopezsanchez (2016). Particle filter approach for real-time estimation of crop phenological states using time series of NDVI images, Remote Sens., 8, 610.

Demirevska-Kepova, K., L. Simova-Stoilova, Z. Stoyanova, R. Holzer and U. Feller, (2004). Biochemical changes in barley plants after excessive supply of copper and manganese, Environ. Exp. Bot., 52, 253-266.

Díaz, S.P. and J.A. Vilar (2010). Comparing Several Parametric and Nonparametric Approaches to Time Series Clustering: A Simulation Study, J Classif., 27, 333-362.

Dunagan, S.C., M.S. Gilmore and J.C. Varekamp (2007). Effects of mercury on visible/near-infrared reflectance spectra of mustard spinach plants (*Brassica rapa* P.), Environ. Pollut., 148, 1, 301-311.

Ekmekçi, Y., D. Tanyolaç, and B. Ayhan (2008). Effects of Cadmium on Antioxidant Enzyme and Photosynthetic Activities in Leaves of Two Maize Cultivars, J. Plant Physiol., 165, 600-611.

Esling, P. and C. Agon (2012). Time-series data mining, ACM Computing Surveys, 45, 1, 1-34.

Estrabou, C., E. Filippini, J.P. Soria, G. Schelotto, and J.M. Rodriguez (2011). Air Quality Monitoring System Using lichens as bioindicators in Central Argentina, Environ. Monit. and Asses., 182, 1-4, 375-83.

Farooqui, A., K. Kulshreshtha, K. Srivastava, S.N. Singh, S.A. Farooqui, V. Pandey and P.J. Ahmad, (1995). Photosynthesis, Stomatal Response and Metal Accumulation in *Cineraria Maritima* L. and *Centauria Moschata* L. Grown in Metal-Rich Soil. Sci, Total Environ., 164, 203-207.

Fluckiger, W., S. Braun, S. Leonardi, N. Asche and R. Fluckiger-Kellhe (1986). Factors contribuing to forest decline in northwestern Switzerland, Tree Physiol., I, 177-181.

Friedland, A.J., A.H. Johnson and T.G. Siccama (1986). Zinc, Cu, Ni and Cd in the forest floor in the northeastern United States, Water Air Soil Poll., 29, 233-243.

Fu, X., Y.L. Zhao, J.H. Li, J.Y. Zeng, Y.Y. Wang, and T.T. He (2013). Research on hyper-spectral remote sensing in heavy metal pollution soil, China Min. Mag., 22, 1, 65-68.

Galeano, P. and D. Peña, (2000). Multivariate Analysis in Vector Time Series. Resenhas, the Journal of the Institute of Mathematics and Statistics of the University of Sao Paolo, 4, 383-403.

Gartner, E.J. (1987). Forest decline in the Federal Republic of Germany. Appearance, extent, potential causes. XIV Intern, Bot. Congr., Berlin, 24 July – 1 Aug., 1987.

Ghosh, M. and S.P. Singh (2005). A review on phytoremediation on heavy metals and utilization of its byproducts, Appl. Eco. Env. Res., 3, 1, 1-18.

Glenn, E.P., A.R. Huete, P.L. Nagler and S.G. Nelson (2008). Relationship between remotely-sensed vegetation indices, canopy attributes and plant physiological processes: What vegetation indices can and cannot tell us about the landscape, Sensors, 8, 2136-2160.

Goetz, S.J. and S.D. Prince (1996). Remote sensing of net primary production in boreal forest stands, Agricultural and Forest Meteorolog., 17, 149-179.

Guan, L. and X. Liu (2009). Experimental research on remote sensing diagnosis method of cd pollution stress in rice, Trans. Chin. Soc. Agric. Eng., 25, 168-173.

Guerrero, L. A., G. Maas, and W. Hogland (2013). Solid waste management challenges for cities in developing countries, Waste Management, 33, 1, 220-232.

Hagemeyer, J. and S.W. Breckle (1996). Growth under trace element stress. In: Waisel Y, Eshel A, Kafkafi U (Editor) Plant roots: the hidden half, 2nd, Dekker, New York, 415-433.

Hasanuzzaman, M., K. Nahar, S. S. Gill, and M.I. Fujita (2014). Drought Stress Responses in Plants, Oxidative Stress,and Antioxidant Defense. In Climate Change and Plant Abiotic Stress Tolerance, First Edition. (Editor) by Narendra Tuteja and Sarvajeet S. Gill.Ó2014 Wiley-VCH Verlag GmbH & Co. KGaA. Published 2014 by Wiley-VCH Verlag GmbH & Co. KGaA, 209-249.

Herrick, G.T. and A.J. Friedland (1991). Winter desiccation and injury of subalpine red spruce, Tree Physiology, 8, 23-36.

Hu, K., Z. Zhang, H. Fang, Y. Lu, Z. Gu and M. Gao (2021). Spatio-Temporal Characteristics and Driving Factors of the Foliage Clumping Index in the Sanjiang Plain from 2001 to 2015, Remote Sens., 13, 2797

Huang, Y., X. Liu, Y. Shen, S. Liu and F. Sun (2015). Advances in Remote Sensing Derived Agricultural Drought Monitoring Indices and Adaptability Evaluation Methods, Trans. Chin. Soc. Agric. Eng., 31, 186-195.

Huang, Z., X. Liu, M. Jin, C. Ding, J. Jiang and L. Wu (2016). Deriving the Characteristic Scale for Effectively Monitoring Heavy Metal Stress in Rice by Assimilation of GF-1 Data with the WOFOST Model, Sensors, 16, 340.

Huete, A.R. (1988). A soil-adjusted vegetation index (SAVI, Remote Sens. Environ., 25, 295-309.

Igbinomwanhia D. and B. Ideho (2014). A Study of the Constraint to Formulation and Implementation of Waste Management Policies in Benin Metropolis, Nigeria, J. Applied Sci. Environ. Manag., 18, 2,197-202.

Innes, J. L. (1993). Forest Health: Its Assessment and Status. Commonwealth Agricultural Bureau, Wallingford, 667.

Ivanov, Y.V., A.V. Kartashov, A.I. Ivanova, Y.V. Savochkin and W. Kuznetsov (2016). Effects of zinc on Scots pine (*Pinus sylvestris* L.) seedlings grown in hydroculture, Plant Physiol. Biochem., 102, 1-9.

Ji, L. and A.J. Peters (2007). Performance Evaluation of Spectral Vegetation Indices Using a Statistical Sensitivity Function, Remote Sens. Environ., 106, 59-65.

Jiang, L., G. Jiapaer, A. Bao, H. Guo and F. Ndayisaba (2017). Vegetation Dynamics and Responses to Climate Change and Human Activities in Central Asia, Sci. Total Environ., 599-600, 967-980.

Jimenez-Ballesta, R., F. García-Navarro, S. Bravo, J. Amoros, C. Perez-de-Los-Reyes and M. Mejías (2017). Environmental assessment of potential toxic trace element contents in the inundated floodplain area of Tablas de Daimiel wetland (Spain), Environ. Geochem. Health, 39, 1159-1177.

Jin, M., X. Liu, L. Wu and M. Liu (2015). An Improved Assimilation Method with Stress Factors Incorporated in the WOFOST Model for the Efficient Assessment of Heavy Metal Stress Levels in Rice, Int. J. Appl. Earth Obs. Geoinformation, 41, 118-129.

Jin, M., X. Liu, L. Wu and M. Liu (2017). Distinguishing heavy-metal stress levels in rice using synthetic spectral index responses to physiological function variations, IEEE J. Sel. Top. Appl. Earth Obs. Remote Sens., 10, 75-86.

Johnson, A., D. Norton, B. Yake and S. Twiss (1990). Transboundary metal pollution of the Columbia River (Franklin D. Roosevelt Lake), Bull. Environ. Contam. Toxicol., 45, 711-717.

Kabata-Pendias, A. and A.B. Mukherjee (2007). Trace Elements from Soil to Human, Springer Berlin, Heidelberg (Editor), 550.

Kancheva, R. and D. Borisova (2007). Vegetation stress indicators derived from multispectral and multitemporal data, Space Technology, 26, 3, 1-8.

Kancheva, R., I. Iliev, D. Borisova, S. Chankova, and V. Kapchina (2005). Detection of plant physiological stress using spectral data", Ecol. Engin. Environ. Protec., 1, 4-9.

Kang, Y., E. Guo, Y. Wang, Y. Bao, Y. Bao and N. Mandula (2021). Monitoring Vegetation Change and Its Potential Drivers in Inner Mongolia from 2000 to 2019, Remote Sens., 13, 3357.

Karbassi, A., S. Tajziehchi and S. Afshar (2015). An investigation on heavy metals in soils around oil field area.ì, Global J. Environ. Sci. Manag., 1, 4, 275-282.

Khalili, R., S. Anvari and M. Honarmand, (2015). Combination Of Biochemical And Hyperspectral Remote Sensing Methods For Detection Of Heavy Metal Pollutions In Eucalyptus Leaves (Case Study: The City Of Bam),The International Archives of the Photogrammetry, Remote Sensing and Spatial Information Sciences, Vol. XL-1/W5, 379-385.

Kooistraa, L., E.A.L. Salasc, J.G.P.W. Cleversc, R. Wehrensb, R.S.E.W. Leuvena, P.H. Nienhuisa and L.M.C. Buydensb, (2004). Exploring field vegetation reflectance as an indicator of soil contamination in river floodplains, Environ. Pollut., 127, 281-290.

Kovalchuk, O., V. Titov, B. Hohn and I. Kovalchuk, (2001). A sensitive transgenic plant system to detect toxic inorganic compounds in the environment, Nat Biotechnol., 19(6), 568-72.

Kozlowski, T.T. and H.A. Constantinidou (1986). Responses of woody plants to environmental pollution. Part I: Sources and types of pollutants and plant responses. Part 11: Factors affecting responses to pollution and alleviation of pollution effects, For. Abstr., 47, 5-51.

Krause, G.H.M., U. Arndt, C.J. Brandt, J. Bucher, G. Kenk and E. Matzner (1986). Forest decline in Europe: development and possible causes. Water, Air, Soil Pollut., 31, 647-668.

Lausch, A., S. Erasmi, D.J. King, P. Magdon and M. Heurich (2017). Understanding Forest Health with Remote Sensing-Part II – A Review of Approaches and Data Models, Remote Sens., 9, 129.

Lausch, A., E. Borg, J. Bumberger, P. Dietrich, M. Heurich, A. Huth, A. Jung, R. Klenke, S. Knapp, H., Mollenhauer, et al. (2018). Understanding Forest Health with Remote Sensing, Part III: Requirements for a Scalable Multi-Source Forest Health Monitoring Network Based on Data Science Approaches. Remote Sens., 10, 1120.

Lei, H. and B. Sun (2007). A Study on the Dynamic Time Warping in Kernel Machines. In 2007 Third International IEEE Conference on Signal-Image Technologies and Internet-Based System, 839-845.

Li, Q., F. Yang, B. Zhang, X. Zhang and G. Zhou (2008). Biogeochemistry responses and spectral characteristics of Rhus chinensis Mill under heavy metal contamination stress (in Chinese). Journal of Remote Sensing, 12, 2, 284-290.

Li, S., J. Xiao, P. Ni, J. Zhang, H. Wang, and J. Wang (2014). Monitoring paddy rice phenology using time series MODIS data over Jiangxi Province, China. Int. J. Agric. Biol. Eng., 7, 28-36.

Li, Q., J. Guo, F. Wang and Z. Song (2021). Monitoring the Characteristics of Ecological Cumulative Effect Due to Mining Disturbance Utilizing Remote Sensing, Remote Sens., 13, 5034.

Liao, T. W. (2005). Clustering of time series data-a survey. Pattern Recognition, 38(11), 1857-1874.

Liu, Y.J., Y.G. Zhu and H. Ding, (2007). Lead and cadmium in leaves of deciduous trees in Beijing, China: development of a metal accumulation index (MAI), Environ Pollut., 145(2), 387-390.

Liu, Y., Y. Li, S. Li and S. Motesharrei (2015). Spatial and Temporal Patterns of Global NDVI Trends: Correlations with Climate and Human Factors, Remote Sens. 2015, 7.

Liu, F., X. Liu, L. Zhao, C. Ding, J. Jiang and L. Wu (2015). The Dynamic Assessment Model for Monitoring Cadmium Stress Levels in Rice Based on the Assimilation of Remote Sensing and the WOFOST Model, IEEE J. Sel. Top. Appl. Earth Obs. Remote Sens., 8, 1330-1338.

Liu, M., X. Liu, B. Zhang and C. Ding (2016). Regional heavy metal pollution in crops by integrating physiological function variability with spatio-temporal stability using multi-temporal thermal remote sensing, Int. J. Appl. Earth Obs. Geoinf., 51, 91-102.

Liu, M., X. Liu, J. Li and T. Li (2012). Estimating Regional Heavy Metal Concentrations in Rice by Scaling up a Field-Scale Heavy Metal Assessment Model, Int. J. Appl. Earth Obs. Geoinfo., 19, 12-23.

Liu, M.L., X.N. Liu, W.C. Ding and L. Wu (2011). Monitoring stress levels on rice with heavy metal pollution from hyperspectral reflectance data using wavelet-fractal analysis. Int. J. Appl. Earth Obs. Geoinfo., 13, 2, 246-255.

Liu, S., X. Liu, M. Liu, L. Wu, C. Ding, and Z. Huang (2017). Extraction of rice phenological differences under heavy metal stress using EVI time-series from HJ-1A/B Data. Sensors, 17, 1243.

Liu, T., X. Liu, M. Liu and L. Wu (2018). Evaluating Heavy Metal Stress Levels in Rice Based on Remote Sensing Phenology, Sensors, 18, 860.

Liu, Y.L., H. Chen, G.F. Wu and X.G. Wu (2010). Feasibility of estimating heavy metal concentrations in Phragmites australis using laboratory-based hyperspectral data-A case study along Le'an River, China, Int. J. Appl. Earth Obs. Geoinf., 12, 166-170.

Llewellyn, G.M., L. Kooistra and P.J. Curran (2001). The red-edge of soil contaminated grassland. In: Proceedings, 8th International Symposium on Physical Measurements and Signatures in Remote Sensing, Aussois, 8-12 January 2001. CNES, Toulouse, 381-386.

Lv, J., Y. Liu, Z. Zhang, R. Zhou and Y. Zhu (2015). Distinguishing Anthropogenic and Natural Sources of Trace Elements in Soils Undergoing Recent 10-Year Rapid Urbanization: A Case of Donggang, Eastern China, Environ. Sci. Pollut. Res., 22, 10539-10550.

Mancino, G., A. Ferrara, A. Padula and A. Nolè (2020). Cross-Comparison between Landsat 8 (OLI) and Landsat 7 (ETM+) Derived Vegetation Indices in a Mediterranean Environment, Remote Sens, 12, 291.

Mancino, G., R. Console, M. Greco, C. Iacovino, M.L. Trivigno and A. Falciano (2022). Assessing Vegetation Decline Due to Pollution from Solid Waste Management by a Multitemporal Remote Sensing Approach, Remote Sens., 14, 428.

Mandzhieva, S.S., T.M. Minkina, V.A. Chaplygin, G. V. Motuzova, S. N. Sushkova, T. V. Bauer and D. G. Nevidomskaya (2016). Plant contamination by heavy metals in the impact zone of Novocherkassk Power Station in the south of Russia, J. Soils Sediments,16, 1383-1391

Martin, J.A.R., C. Gutiérrez, M. Torrijos and N. Nanos (2018). Wood and bark of Pinus halepensis as archives of heavy metal pollution in the Mediterranean Region, Environ. Pollut., 239, 438-447.

Massadeh, A.M., Q.M. Jaradat, K.A. Momani and M.A. Saleem (2009). Distribution of Heavy Metals in Some Tree Leaves along the Main Road in an Agricultural Area, Commun. Soil Sci. Plant Analys, 40, 1254-1267.

Mathur, S., H.M. Kalaji and A. Jajoo (2016). Investigation of deleterious effects of chromium phytotoxicity and photosynthesis in wheat plant, Photosynthetica, 54, 185-192.

McGwire, K., M. Friedl and J.E. Estes (1993). Spatial Structure, Sampling Design and Scale in Remotely-Sensed Imagery of a California Savanna Woodland, Int. J. Remote Sens., 14, 2137-2164.

McLaughlin, S. B. (1985). Effects of air pollution on forests. A critical review, J. Air Pollut. Control Assoc., 35, 512-534.

Mera, R., E. Torres and J. Abalde (2016). Influence of sulphate on the reduction of cadmium toxicity in the microalga *Chlamydomonas moewusii*, Ecotoxicol. Environ. Saf., 128: 236-245.

Milton, N.M., C.M. Ager, B.A. Eiswerth and M.S. Power, (1989). Arsenic and selenium induced changes in spectral reflectance and morphology of soybean plants. Remote Sens. Environ., 30, 263-269.

Minkina, T.M., G.V. Motuzova, O.G. Nazarenko, V.S. Kryshchenko and S.S. Mandzhieva, (2008) Forms of heavy metal compounds in soils of the Steppe Zone, Eurasian Soil Sci, 41, 7, 708-716.

Mirsal, I. (2004). Soil pollution. Origin, monitoring & remediation. Berlin, Germany: Springer-Verlag (Editor), 242.

Möller-Levet, C.S., F. Klawonn, K. Cho and O. Wolkenhauer (2003). Fuzzy Clustering of Short Time-Series and Unevenly Distributed Sampling Points. In Proceedings of the 5th International Symposium on Intelligent Data Analysis, 2810, 330-340.

Müller-Wilm, U. (2016a). Sentinel-2 MSI – Level-2A Prototype Processor Installation and User Manual. S2PAD-VEGA-SUM-0001, 2.2, 51.

Müller-Wilm, U. (2016). Sen2Cor 2.2.1 – Software Release Note. ESA-EOPG-CSCGS-TN-0014, Issue 1.0.

Myneni, R.B., C.D. Keeling, C. Tucker, J.G. Asrar and R.R. Nemani (1997). Increased plant growth in the northern latitudes from 1981-1991, Nature 386, 698-702.

Odumo, B., G. Carbonell, H. Angeyo, J. Patel, M. Torrijos and J. Rodríguez Martín (2014). Impact of gold mining associated with mercury contamination in soil, biota sediments and tailings in Kenya, Environ. Sci. Pollut. Res., 21, 12426-12435.

Montero, P. and J.A. Vilar (2014). TSclust: An R Package for Time Series Clustering, J. Stat. Softw., 62, 1, 1-43.

Napa, Ü., I. Ostonen, N. Kabral, K. Kriiska and J. Frey (2017). Biogenic and contaminant heavy metal pollution in Estonian coniferous forests, Reg. Environ. Change, 17, 2111-2120.

Patel, K.S., R. Sharma, N.S. Dahariya, A. Yadav, B. Blazhev, L. Matini and J. Hoinkis (2015). Heavy Metal Contamination of Tree Leaves, Am. J. Analyt. Chem., 6, 687-693.

Peñuelas, J., I. Filella, and J. A. Gamon (1995). Assessment of photosynthetic radiation-use efficiency with spectral reflectance, The new phytologist, 131, 291-296.

Petrotou, A., K. Skordas, G. Papastergios and A. Filippidis (2012). Factors affecting the distribution of potentially toxic elements in surface soils around an industrialized area of northwestern Greece, Environ. Earth Sci., 65, 823-833.

Pettorelli, N., J.O. Vik, A. Mysterud, J.M. Gaillard and C.J. Tucker (2005). Using the satellite-derived NDVI to assess ecological responses to environmental change, Trends Ecol. Evol., 20, 503-509.

Piczak, K., A. Lesniewicz and W. Zyrnicki (2003). Metal Concentrations in Deciduous Tree Leaves from Urban Areas in Poland, Environmental Monitoring and Assessment, 86, 273-287.

Pierart, A., M. Shahid, N. Sejalon-Delmas and C. Dumat (2015). Antimony bioavailability: knowledge and research perspectives for sustainable agricultures, J. Hazard Mater, 289, 219-234.

Pree, H., B. Herwig, T. Gruber, B. Sick, K. David and P. Lukowicz (2014). On general purpose time series similarity measures and their use as kernel functions in support vector machines, Info. Sci., 281, 478-495.

Rahman, M.A., H. Hasegawa, M.M. Rahman, M.N. Islam, M.A.M. Miah and A. Tasmen (2007). Effect of arsenic on photosynthesis, growth and yield of five widely cultivated rice (*Oryza sativa* L.) varieties in Bangladesh, Chemosphere, 67, 1072-1079.

Ren, H.Y., D.F. Zhuang, J.J. Pan, X.Z. Shi and H.J. Wang (2008). Hyper-spectral remote sensing to monitor vegetation stress, J. Soils Sedim., 8, 323-326.

Rodríguez Martín, J.A., J.A.R. Martín, C.D. Arana, J.J. Ramos-Miras, C. Gil, and R. Boluda (2015). Impact of 70 years urban growth associated with heavy metal pollution, Environ. Pollut., 196, 156-163.

Rodríguez Martín, J.A. and N. Nanos (2016). Soil as an Archive of Coal-Fired Power Plant Mercury Deposition, J. Hazard. Mater., 308, 131-138.

Rumpf, T., A.K. Mahlein, U. Steiner, E.C. Oerke, H.W. Dehne and L. Pluemer (2010). Early detection and classification of plant diseases with support vector machines based on hyperspectral reflectance, Comput. Electron. Agr., 74, 1, 91-99.

Sabir, M., E.A. Waraich, K.R. Hakeem, M. Öztürk, H.R. Ahmad and M. Shahid (2015). Phytoremediation: Mechanisms and adaptations, Soil Remediat Plants, 4, 85-105.

Sanches, I.D., C.R. Souza Filho and R.F. Kokaly (2014). Spectroscopic Remote Sensing of Plant Stress at Leaf and Canopy Levels Using the Chlorophyll 680nm Absorption Feature with Continuum Removal, ISPRS J. Photogramm. Remote Sens., 97, 111-122.

Schreck, E., Y. Foucault, G. Sarret, S. Sobanska, L. Cécillon, M. Castrec-Rouelle, G. Uzu, and C. Dumat (2012). Metal and metalloid foliar uptake by various plant species exposed to atmospheric industrial fallout: mechanisms involved for lead, Sci. Total Environ., 427-428, 253-262.

Schutt, P. and E.B. Cowling (1985). Waldsterben, a general decline of forests in Central Europe: symptoms, development, and possible causes, Plant Disease, 69, 518-558.

Scudiero, E., T.H. Skaggs and D.L. Corwin (2015). Regional-scale soil salinity assessment using Landsat ETM plus canopy reflectance, Remote Sens. Environ., 169, 335-343.

Shahid, M., E. Pinelli, B. Pourrut, J. Silvestre, and C. Dumat (2011). Lead-induced genotoxicity to *Vicia faba* L. roots in relation with metal cell uptake and initial speciation, Ecotoxicol. Environ. Saf., 74, 78-84.

Shahid, M., C. Dumat, J. Silvestre and E. Pinelli (2012). Effect of fulvic acids on lead-induced oxidative stress to metal sensitive *Vicia faba* L. plant, Biol. Fert. Soils, 48, 689-697.

Shahid, M., E. Ferrand, E. Schreck, and C. Dumat (2013). Behavior and impact of zirconium in the soil-plant system: Plant update and phytotoxicity, Rev. Environ. Contam. Toxicol., 221, 107-127.

Shahid M., A. Austruy, G. Echevarria, M. Arshad., M. Sanaullah, M. Aslam, M. Nadeem, W. Nasim and C. Dumat (2014). EDTA-Enhanced Phytoremediation of Heavy Metals: a Review, Soil and Sediment Contamination: An International Journal, 23(4), 389-416.

Shiyab, S., J. Chen, F.X. Han, D.L. Monts, F.B. Matta, M. Gu and Y. Su (2009). Phytotoxicity of mercury in Indian mustard (*Brassica juncea* L.), Ecotoxicology Environ. Safety, 72, 619-625.

Singh, M., P. Goel and A.K. Singh (2005). Biomonitoring of Lead in Atmospheric Environment of An Urban Center of the Ganga Plain, India, Environ Monit Assess., 107, 101-114.

Singh, J. and A.S. Kalamdhad (2011). Effects of Heavy Metals on Soil, Plants, Human Health and Aquatic Life, Int. J. Res. Chem. Environ., 1, 15-21.

Singh, V., B.N. Tripathi and V. Sharma (2015). Interaction of Mg with heavy metals (Cu, Cd) in *T. aestivum* with special reference to oxidative and proline metabolism, J. Plant Res., 129, 487-497.

Singha, M., B. Wu and M. Zhang (2016). An object-based paddy rice classification using multi-spectral data and crop phenology in Assam, Northeast India. Remote Sens., 8, 479.

Slaton, M.R., E.R. Hunt and W.K. Smith (2001). Estimating near-infrared leaf reflectance from leaf structural characteristics, Am. J. Botany, 88, 278-284.

Smith, W.H. (1970). Air pollution: effects on the structure and function of the temperate forest ecosystem. Environ. Pollut., 6, 2, 111-129.

Sridhar, B.B.M., F.X. Han, S.V. Diehl, D.L. Monts and Y. Su (2007). Spectral reflectance and leaf internal structure changes of barley plants due to phytoextraction of zinc and cadmium, Int. J. Remote Sens., 28, 1041-1054.

Steffan, J.J., E.C. Brevik, L.C. Burgess and A. Cerdà (2018). The effect of soil on human health: an overview, Eur. J. Soil Sci., 69, 1, 159-171.

Stankovic, S. and A.R. Stankovic (2013). Chapter 5: Bioindicators of Toxic Metals. In: Lichtfouse, E., Schwarzbauer, J. and Robert, D., (Editor)., Green Materials for Energy, Products and Depollution, Series Volume 3, Springer Netherlands, 151-228.

Su, Y., B.B. M. Sridhar, F.X. Han, S.V. Diehl and D.L. Monts (2007). Effect of bioaccumulation of Cs and Sr natural isotopes on foliar structure and plant spectral reflectance of Indian mustard (*Brassica juncea*), Water, Air, and Soil pollution, 180, 65-74.

Temmerman, L.D., J. Nigel, B. Bell, J.P. Garrec, A. Klumpp, G.H.M. Krause and A.E.G. Tonneijck (2005). Biomonitoring the Ganga Plain, India, Environ. Monit. Asses., 107, 101-114.

Tomaševic, M., S. Rajšic, D. Dorđević, M. Tasić, J. Krstić and V. Novaković (2004). Heavy Metals Accumulation in Tree Leaves From Urban Areas, Environ. Chem. Lett., 2, 151-154.

Wang H.Y., M. Klatte, M.H. Jakoby Bäumlein, B. Weisshaar and P. Bauer (2007). Iron deficiency-mediated stress regulation of four subgroup Ib BHLH genes in *Arabidopsis thaliana*., Planta, 226, 897-908.

Wang, D. and X. Liu (2018). Comparative Analysis of GF-1 and HJ-1 Data to Derive the Optimal Scale for Monitoring Heavy Metal Stress in Rice, Int. J. Environ. Res. Public Health, 15, 3, 461.

Wang, X., A. Mueen, H. Ding, G. Trajcevski, P. Scheuermann and E. Keogh (2012). Experimental comparison of representation methods and distance measures for time series data. Data Mining and Knowledge, Discovery, 26, 2, 275-309.

Wani, P.A., M.S. Khan and A. Zaidi (2008). Effects of Heavy Metal Toxicity on Growth, Symbiosis, Seed Yield and Metal Uptake in Pea Grown in Metal Amended Soil, Bull. Environ. Contam. Toxicol., 81, 152-158.

Wei, S., B.M. Chen and L. Lin (2013). Soil heavy metal pollution of cultivated land in China, Res. Soil Water Conserv., 20, 293-298.

Wevers, J., D. Müller, J. Scholze, G. Kirches, R. Quast and C. Brockmann (2021). IdePix for Sentinel-2 MSI Algorithm Theoretical Basis Document. Online: https://zenodo.org/record/5788067#.YmucodpByUk

Xiong, T., T. Leveque, M. Shahid, Y. Foucault, S. Mombo and C. Dumat (2014). Lead and cadmium phytoavailability and human bioaccessibility for vegetables exposed to soil or atmospheric pollution by process ultrafine particles, J. Environ. Qual., 43,1593-1600.

Xu, L.L., Z.Y. Fan, Y.J. Dong, J. Kong and X.Y. Bai (2014). Effects of exogenous salicylic acid and nitric oxide on physiological characteristics of two peanut cultivars under cadmium stress, Biol. Plant., 59, 171-182.

Yoder, B.J. and R.H. Waring (1994). The normalized difference vegetation index of small Douglas-fir canopies with varying chlorophyll concentrations, Remote Sens. Environ., 49, 81-91.

Zaanouni, N., M. Gharssallaoui, M. Eloussaief and S. Gabsi (2018). Heavy metals transfer in the olive tree and assessment of food contamination risk, Environ. Sci. Pollut. Res., 25, 18320-18331.

Zhang, J.-H. and M. Hang (2009). Eco-toxicity and metal contamination of paddy soil in an e-wastes recycling area, J. Hazard. Mater., 165, 744-750.

Zhang, Z., M. Liu, X. Liu and G. Zhou (2018). A New Vegetation Index Based on Multitemporal Sentinel-2 Images for Discriminating Heavy Metal Stress Levels in Rice, Sensors, 18, 2172.

Zhao, L., Y. L. Sun, S.X. Cui, M. Chen, H.M. Yang, H.M. Liu, T-Y Chai and F. Huang (2011). Cd-induced changes in leaf proteome of the hyperaccumulator plant *Phytolacca americana*, Chemosphere, 85, 56-66.

Zhao, S., X. Qian, X. Liu and Z. Xu (2018). Finding the Key Periods for Assimilating HJ-1A/B CCD Data and the WOFOST Model to Evaluate Heavy Metal Stress in Rice, Sensors, 18, 1230.

Zhou, G., X. Liu, S. Zhao, M. Liu and L. Wu (2017). Estimating Fapar of rice growth period using radiation transfer model coupled with the WOFOST model for analyzing heavy metal stress, Remote Sens., 9, 424.

Zhu, X., S. Zhang, T. Liu and Y. Liu (2021). Impacts of Heat and Drought on Gross Primary Productivity in China, Remote Sens., 13, 378.

Zouari, M., C. Ben Ahmed, N. Elloumi, K. Bellassoued, D. Delmail, P. Labrousse, F. Ben Abdallah and B. Ben Rouina (2016). Impact of Proline Application on Cadmium Accumulation, Mineral Nutrition and Enzymatic Antioxidant Defense System of *Olea Europaea* L. Cv Chemlali Exposed to Cadmium Stress, Ecotoxicol. Environ. Saf., 128, 195-205.

Zouari, M.; Ch. Ben Ahmed, W. Zorrig, N. Elloumi, M. Rabhi, D. Delmail, B. Ben Rouina, P. Labrousse and F. Ben Abdallah (2016). Exogenous Proline Mediates Alleviation of Cadmium Stress by Promoting Photosynthetic Activity, Water Status and Antioxidative Enzymes Activities of Young Date Palm (*Phoenix Dactylifera* L.), Ecotoxicol. Environ. Saf., 128, 100-108.

***CORRESPONDING AUTHOR: Giuseppe MANCINO**,
Centro di Geomorfologia Integrata per l'Area del Mediterraneo, Via F. Baracca 175, 85100 Potenza, Italy
e-mail: g.mancino@cgiam.org